Overhead Lines and Weather

<div style="text-align: right">**7**</div>

Svein Fikke

Contents

S. Fikke (✉)
Lørenskog, Oslo, Norway
e-mail: fikke@metconsult.no

7.1   Introduction

Electric overhead lines are built and run through any type of terrain, from the maritime coast to the continental inland, from sea level to high mountains, and also in some of the most challenging climate zones of the world from rain forests to deserts, from tropical zones to the arctic. They are exposed to a wide variety of weather impacts like bush fires, extreme heat, sandstorms, typhoons, tornadoes, lightning, extratropical weather systems, sprays of sea salt, freezing rain, rime icing, wet snow, floods, etc. It is therefore of critical significance that such lines are designed in a secure manner to be prepared for any type of weather event and impact which otherwise could disrupt their reliable operation and cut off the expected supply of electric power to the society at its delivery point. On the other hand, it is likewise important that such lines are not built stronger and more expensively than they need to be, in order not to overinvest in more security than needed and also to avoid structures that are much heavier and visually more predominant than the public can or will accept.

There are many design codes and standards available for buildings and structures to cover loadings from strong winds, snow on ground, earthquakes, etc. (See for instance: ASCE (2009), CAN/CSA (2010), EPRI (2008), IEC TR 60826 (2003), NESC (2007), AS/NZ (1999) and the series of CEN EN 1991–1 for Europe.). Such codes and standards are likewise applicable for individual towers and masts for electric overhead lines. However, most of these building codes are developed for singular buildings or structures located in populated areas where adequate environmental data are available. Electric overhead lines frequently run through very remote and complex terrain where such conventional standards and codes have limited relevance. Accordingly, international standardisation bodies for the electric power industries (IEC, CENELEC, ASCE, AS/NZS and others), as well as many countries with particular needs, have established international and national codes to cover most of the needs for the development of their electric overhead grids. It is still however especially important to have a critical view on local weather effects along the line routes and what additional information and data are needed when a line is planned through unknown terrain where little or no adequate experiences may exist.

Such topics have been addressed by many Cigré SC B2 working groups for many decades. Especially the development of the IEC TR 60826 "Designing criteria for overhead transmission lines" has focused on the variety of environmental influences on design and operation of electric overhead power lines. This chapter is focusing on the learning from several Cigré TB, especially those dealing with atmospheric icing and various wind phenomena with particular reference to overhead lines in exposed terrain and climate.

Intentionally, this chapter contains only few references to standards, design codes, textbooks, etc., except current Cigré publications with some updates. This is mainly because, like many other fields of science, the science of meteorology is developing very fast, most due to the rapid increase in computer capacities together with direct and remote measurement technologies, especially from automatic sensors, weather radars, satellites, etc. Hence, the 3-dimensional physical and dynamical models of the Earth system, consisting of oceans, atmosphere and cryosphere (floating ice and glaciers) are constantly improving, leading to better weather forecasts and analyses, indeed also for the atmospheric boundary layer in complex mountain terrain.

Table 7.1 Cigré TB which have been used as background documents for this chapter

TB	WG	Title
179	22.06.01	Guidelines for field measurement of ice loadings on overhead line conductors (2001)
256	B2.16	Report on current practices regarding frequencies and magnitude of high intensity winds (2004)
291	B2.16	Guidelines for meteorological icing models, statistical methods and topographical effects (2006)
299	B2.12	Guide for selection of weather parameters for bare overhead conductor ratings (2006)
350	B2.06.09	How overhead lines respond to localized high intensity winds (2008)
410	B2.16	Local wind speed-up on overhead lines for special terrain features (2010)
438	B2.29	Systems for prediction and monitoring of ice shedding, anti-icing and de-icing for overhead power line conductors and ground wires (2010)
	B2.28	Meteorological data and analyses for assessing climatic loads on OHLs (Cigré TB 645, 2015)
485	B2.29	Overhead Line Design Guidelines for Mitigation of Severe Storm Damage (2014)

This chapter therefore deals with the main topics of weather impacts on overhead lines in more general terms, and referring to Cigré SCB2 TB where more information is found. For more specific questions and applications the reader is recommended to identify necessary updates at national weather services in order to be updated on particular needs, if they are not otherwise found in newer Cigré publications.

The main Cigré TBs referred to in this chapter are listed in Table 7.1.

This chapter does not discuss other second order effects from extreme weather, like heat waves, bush fires, floods, avalanches, lightning, sea salt, desert dust, etc., as these phenomena are treated elsewhere in both in Cigré SCs and National codes. A short comment on the combined effect of icing and pollution is however given.

Finally, this chapter summarizes some updated knowledge on global change issues relevant for overhead lines.

7.2 Wind

7.2.1 Overview

Many different wind systems are prevailing over the earth, depending on geographical location and differences in topography. Many of these wind systems have different names according to local or regional practices, but are often physically of similar nature. According to Cigré B2 TB 256 "Report on current practices regarding frequencies and magnitude of high intensity winds" (2004) the most characteristic wind systems are described as:

- Synoptic or extratropical storms
- (Sub-) Tropical wind systems, such as tropical cyclones, hurricanes, typhoons, etc.

- High intensity winds related to well-developed thunderstorms (supercells) tornadoes, twisters, downbursts, etc.
- Special wind systems, such as katabatic winds, bora, föhn, etc.

Especially in complex or mountainous (alpine) terrain the topography will influence both the mean wind speeds and the turbulence of the wind flow. Such topics are dealt with in Cigré TB 410 "Local wind speed-up on overhead lines for special terrain features" (2010). A particular feature not commonly recognised is that the gust wind speeds will often be higher on the leeward side of a steep mountain side compared to the windward side or over flat terrain. This phenomenon has taken down many power lines and buildings where such damages were not expected.

All these wind patterns are dealt with in these Cigré TBs, and their main topics are summarized in this chapter.

An important issue for dynamic line rating (DLR) is low wind speed and its related thermally driven turbulence. This is not yet (2014) fully treated in a Cigré TB. However, this is an example where there is on-going research in many countries. Therefore it is recommended to seek updated information at the time when such knowledge should be needed.

7.2.2   Extratropical Cyclones (after Cigré TB 256)

Extratropical storms, or polar front cyclones, are formed on the "Polar front" which persists as a sharp divide into the atmosphere between cold, arctic air on the polar side and warmer and more humid air on the tropical side. This frontal divide is circumpolar, in general undulating around 60° on the northern hemisphere. (It is connected to the "jet stream" in the higher atmosphere.) The polar front is normally in a situation of unstable equilibrium (like a small ball resting on the top of a larger ball.) Following a disturbance on this front, a cyclone, or low pressure system, is formed where the warm, sub-tropical air penetrates as a wedge (warm sector) into the colder air mass and slides over the colder, downwind air (warm front), like sliding up on an inclined plane. On the rear side, the colder air penetrates into the warmer air like a sail (cold front). Simultaneously the air pressure near the surface of the earth is lowered.

A typical example of such a system is illustrated in Figure 7.1.

The diameter of these cyclonic systems ranges between 500 and 3000 km, the smaller ones being often the most intense. In the North Atlantic region they start as small disturbances outside the eastern coast of North America and reach the strongest stage usually as they reach the north-eastern side of the Atlantic and the coastal states of northern Europe from France to the Nordic countries.

The wind then blows counter clock-wise around the depression in the northern hemisphere, and clockwise in the southern, with a minor component towards the centre due to the friction forces from the surface. The stronger the pressure gradient is (from the centre of the depression to the surrounding air), the stronger is the wind speed.

These systems move in a general West to East direction and increase in translation speed as they develop, often achieving translation speeds up to 40 km/hour. The
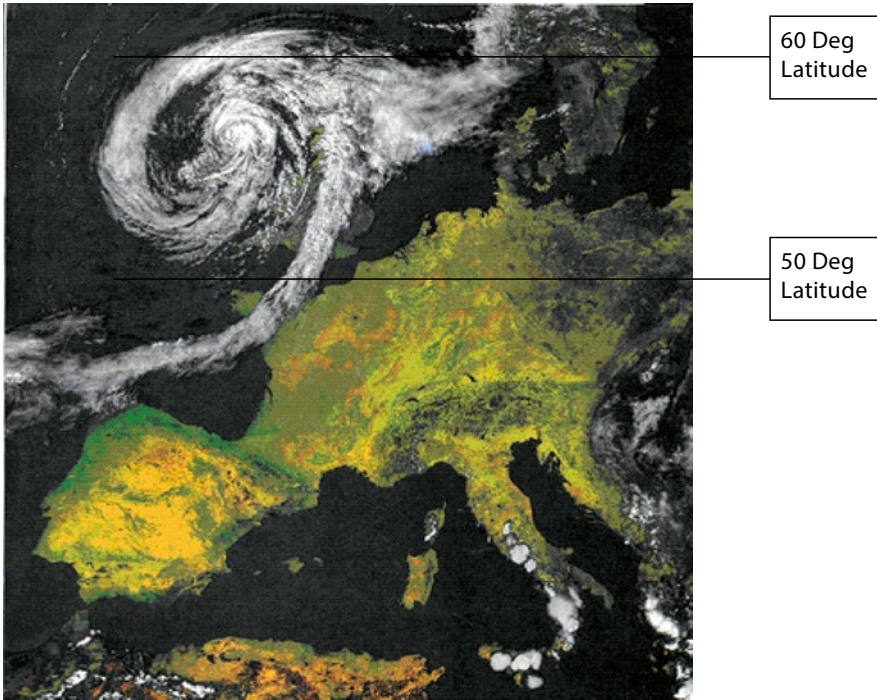
60 Deg
Latitude

50 Deg
Latitude

Figure 7.1 Satellite Image of Extratropical Storm in Northern Europe. The low pressure centre is over Ireland, while the warm front lies over Southern Norway and the cold front stretches over the British Channel, Bretagne and the Bay of Biscay. Thunderstorm activity is also evident over Italy (Photograph Ref Munich RE).

most gusty winds occur along the cold front, where a sharp change in wind direction often also is found (from WSW to NW on the northern hemisphere and from WSW to SW on the southern hemisphere). Also very intense shower clouds (Cumulonimbus, sometimes with thunderstorm cells) form along this cold front.

The energy connected to such fronts is connected to both the jet stream aloft and the sea temperature. The most intense cyclones occur in the months of October to January in the northern hemisphere. The gust wind speeds may exceed 50 to 60 m/s over sea or exposed land areas, mostly in northern regions.

Storm fronts that develop in the southern Antarctic ocean region occur over more expansive areas of ocean at low temperature, and as such tend to be predominately frontal rather that cyclonic. The impact of these southern storm fronts, with wind velocities in the range indicated above, are limited to those land masses around latitude 40 degree S.

Within the western Pacific Region, the Japanese Archipelago is located in the boundary of cold air and warm air currents, and strong winds from extratropical cyclones can also be frequently observed, but wind velocities under such a situation are significantly lower than those of typhoons that also occur.

Due to the large extension of such wind systems they are easily identified by regular meteorological observation networks ("synoptic scale") as well as by the regular weather forecasting models. Accordingly, where such wind systems are prevailing, there are generally well developed statistics for wind speeds and wind directions available for mechanical design of electrical overhead lines as well as for other structures on National levels.

7.2.3   (Sub-)Tropical Wind Systems

Tropical cyclones/hurricanes and hurricanes are also of "synoptic scale" and have potentially very severe low pressure weather systems that affect the tropical coastal regions during the summer months. The strict definition of a tropical cyclone (WMO 1995) is:

> *A non-frontal cyclone of synoptic scale developing over tropical waters and having a definite organized wind circulation with average wind of 34 knots (17.5 m/s) or more surrounding the sustained winds at the centre.*

The tropical cyclone is an intense tropical low pressure weather system where, in the southern hemisphere, winds circulate clockwise around the centre. In Australia, such systems are upgraded to severe tropical cyclone status (referred to as hurricanes or typhoons in some countries) when average, or sustained, surface wind speeds exceed 34 m/s. The accompanying shorter-period destructive wind gusts are often 50 per cent or more higher than this value. These high winds have a buffeting characteristic where the level of 'gustiness' can last for several hours from one direction, only to be followed shortly afterwards by winds of a similar but marginally less magnitude from the opposite direction as the eye of the storm passes a given point.

There are three components of these tropical events that combine to make up the total hazard - strong winds, intense rainfall and induced ocean effects including extreme waves, currents, storm surge and resulting storm tide. The destructive force of these storms is usually expressed in terms of the strongest wind gusts experienced. Maximum wind gust is related to the central pressure and structure of the system, whilst extreme waves and storm surge, are linked more closely to the combination of the mean surface winds, central pressure and regional bathymetry. Satellite photos of tropical cyclone "Fran" approaching Queensland, Australia, in March 1992 is shown in Figure 7.2, and typhoon "Lupi" approaching the coasts of Korea and Japan on 02 December 2003 is shown in Figure 7.3.

Hurricanes in the American region have similar characteristics to those in the Pacific. Experience in recent times in the eastern coastal region of the USA around the state of Florida resulted in significant damage to infrastructure. As an example a satellite photo of the hurricane Katrina, which caused catastrophic damage in New Orleans in August 2005, is shown in Figure 7.4.

Figure 7.2 Tropical
cyclone Fran approaching
the Queensland coast in
March 1992. Note the
clockwise rotation on the
Southern Hemisphere
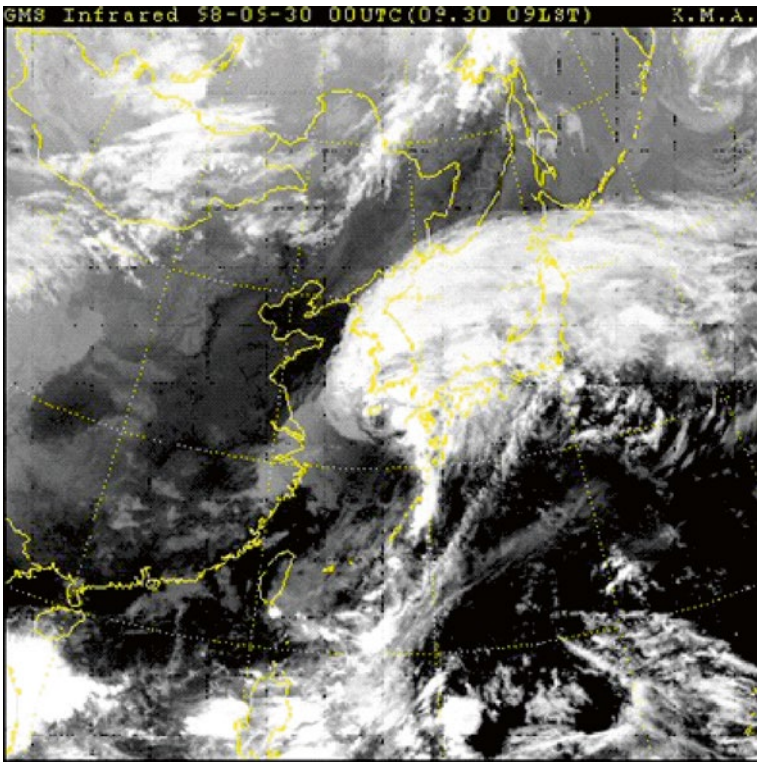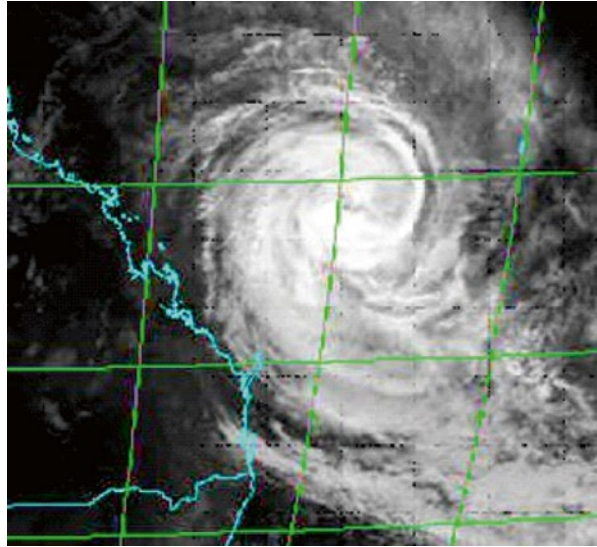(Photograph Bureau of
Meteorology – Australia).

Figure 7.3 Satellite image of Typhoon "Lupi" 2 December 2003 approaching the coasts of Korea
and Japan.

Figure 7.4 Satellite photo of Hurricane Katrina in the Gulf of Mexico, August 2005. Highest wind speed recorded: 280 km/hr, or nearly 80 m/s (Wikipedia).

7.2.4   High Intensity Winds Connected to Thunderstorms

Thunderstorms form in very unstable air masses, with cold air high up in the atmosphere and warm and humid air prevails near the surface of the Earth. When warm air start to "bubble" upwards from the surface it is cooled at the so-called adiabatic laps rate (0,98 °C/100 m for dry air) up to a level where the water vapour condenses, and a cloud is formed above. This condensation releases the "latent heat of evaporation" and this heat will slow down the lapse rate, and hence the air "bubble" will be even warmer than the surrounding air, and accordingly increase its vertical velocity. To compensate for the "lack" of air near ground, there will also be a strong downward wind within the cell (down-draughts). This is the basic principle of formation of a cumulonimbus cloud. Figure 5 shows a sketch of such a well developed thunderstorm cell.

As indicated in Figure 7.5, funnel clouds and eventually tornadoes may develop underneath the leading edge of such a thunderstorm. The visible funnel actually develops from ground, when dust is sucked upwards, or water vapour condenses on its way upwards. The strong winds connected to such tornadoes have a much wider diameter than the visible funnel itself. One example of a tornado with a visible funnel cloud is shown in Figure 7.6.

Well developed thunderstorms are also associated with strong circulating winds around the cell near the ground (clock-wise in the Southern Hemisphere and counter clock-wise in the Northern). However, except for the tornadoes, the strongest wind gusts are often connected to gust fronts connected to the strong down-draughts (down-bursts) as indicated in Figure 7.5.
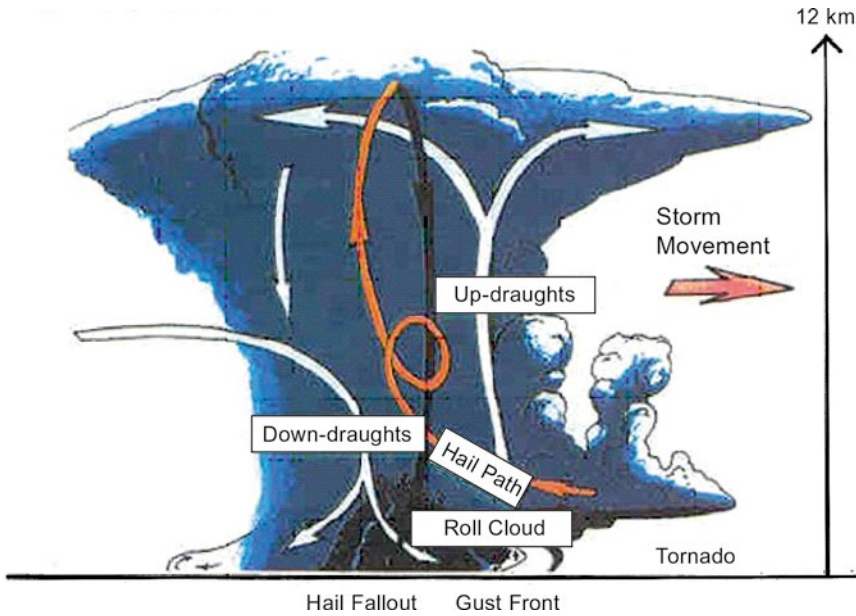
Figure 7.5 Schematic illustration of a mature supercell thunderstorm (Courtesy of Bureau of Meteorology, Australia).

Figure 7.6 Typical funnel cloud associated with a tornado (Photo: Bureau of Meteorology, Australia).

    Due to the small horizontal scale of such phenomena there are generally very limited data for wind speeds associated with tornadoes. Also, they strike at different locations from time to time, and therefore it is very difficult to establish ordinary extreme wind statistics for design purposes of such winds. Due to the catastrophic damages such winds often are connected with, there is generally no demand or wish either to design overhead lines to withstand such wind forces, but rather to handle

the consequences resulting from them in other manners. Countries where such winds occur have therefore developed their own procedures for such consequences these may have on their overhead line networks. See (Cigré TB 256) and (Cigré TB 350) for more details.

Cigré TB 256 also contains classification of these kinds of winds as they are defined in many countries.

7.2.5   Special Wind Systems (after Cigré TB 256)

Other sub-synoptic wind systems are frequently formed on the surface of the Earth, mostly due to strong temperature gradients, either vertically from ground surface and upwards, or horizontally along the surface when cold air may be trapped in (often high level) basins.

Small scale, tornado-like "dust devils" often occur over heated land surface, especially in the afternoon, in tropical or sub-tropical areas when intense sunshine on dry ground has created a strong thermal instability in the lowest 1–200 m of the atmosphere. Although these may reach high wind speeds near their centres, they seldom create significant damage due to their limited extension.

Another phenomenon, similar in principle, often occurs in the Arctic when cold air masses flow out from the arctic ice cover over the open sea in the North Atlantic and Polar Basin. Here the temperature differences may easily be more than 40 °C, and this may give rise to instability depressions in those areas. The wind speeds may be very high in these depressions and therefore cause severe damage to fishing vessels operating in such waters, and they may also hit the coasts of the Northern countries. Nowadays they are detected by satellites and are therefore better forecasted.

Under certain conditions of atmospheric stability, so-called katabatic winds occur in Alpine regions, both in Europe, South America, New Zealand, and other regions with similar charactersitics (Cigré TB 256). Katabatic winds develop on the leeward side of mountains and ridges where the air mass approaching on the windward side is colder than that on the leeward side. Due to its higher density the cold air plunges down from the ridge of a mountain range into the valley below, and can develop speeds of up to 60 m/s in extreme cases, and have devastating effects on overhead lines hit by them. The wind velocity of these winds increases with temperature differentials and mountain or fall height. The velocity is also increased when the wind currents are in the same direction.

One example of such a katabatic wind is in South Eastern Europe called *Bora*. Figure 7.7 shows an example the action of such a wind on an overhead line in Croatia.

Another well-known wind system of the same nature in mountain regions is the föhn wind. A characteristic property of föhn wind is that moist air is lifted over a mountain range where the water vapour is condensed and rains out on the windward side and hence releases the latent heat of condensation, while on the leeward side the air subsides at the dry adiabatic lapse rate and accordingly the air may be much warmer on this side. The föhn wind may also be relatively strong on the leeward side.

Figure 7.7 Conductors blow out during a Bora event in Croatia, January 2003. From Cigré TB 256 (Photo: F. Jakl).

7.2.6 Topographical Effects

Standard codes for wind engineering and design of structures include general rules for speed-up of winds over hills and escarpments and will provide the general wind engineering requirements for design of electrical overhead power lines. They consider mostly homogenous terrain, of various roughness factors, and certain idealised topographical features of two dimensions. There are however limitations for the application of these general rules for treating extreme terrain roughness, predominant hill forms and escarpments, such as many high and steep hills, mountains, valleys and fjords. As many overhead lines in mountain terrain will experience particular, and mostly unexpected, impacts of such phenomena it is important to improve the knowledge of them and how they may interact with an overhead line. Such topographic features may have length scales ranging from a few tens of metres up to several km.

Gust factors in the range of 1.8 - 1.9 (relative to 10 minute mean wind) may apply for wind speeds in such areas at 10 m height above ground. For comparison it can be mentioned that observations of high wind damage during tropical cyclones in Northern Queensland indicate that speed-up effects can also occur during high winds on the upper slopes and crests of coastal mountain range escarpments. Analysis of damage patterns suggest a speed-up of 20 % can occur frequently. The upper level of amplification of this speed-up is dependent on the escarpment slope profile, height and basic wind velocity. The AS/NZS 1170.2 Wind Actions (1999) provides for values of up to 50 %.

The introduction of probabilistic methods has especially encouraged more direct knowledge of any impact of nature on overhead lines.

Some examples of wind enhancements are found in places like:

- over hill crests
- near sharp edges (escarpments) exposed to high level winds over surrounding terrain
- behind elongated mountains (rotor formation)
- behind steep mountain sides (or edges) where particular turbulence may be formed (vortex "streets").
- on the side of hills and mountains (corner effect)
- in valleys (including converging mountains) or fjords where the airflow may be compressed locally (funnelling effect)
- katabatic winds like föhn and bora.

The wind enhancement over hill crests and escarpments are mostly implemented in standard wind codes. These phenomena are based on mechanical flow patterns. Aerodynamical phenomena such as rotors and vortex shedding (streets) are generally not considered in wind codes, although their magnitude may be very substantial. Some of these phenomena are very site specific and can hardly be treated in a wind code format. It was the intention of Cigré TB 410 "Local wind speed-up on overhead lines for specific terrain features" (WG B2.16, April 2010) to give a physical background for some of them and also to suggest a generalized method to handle vortex streets behind steep mountains.

Two well-known examples of small scale dynamic features are also referred to in Cigré TB 410, namely the leeward screw formed rotor behind the Rock of Gibraltar shown in Figure 7.8. In South-westerly winds this rotor introduces a strong perpendicular wind over the runway of the Gibraltar airport (point "B" in Figure 7.8), and also creates dangerous turbulence for low flying aircraft in that area.

Another example is from the island Ailsa Craig in the Firth of Clyde in Scotland, see Figure 7.9. This island is a bit elongated and the highest point is about 350 m.

Figure 7.8 A leeward screw formed rotor from the Rock of Gibraltar.

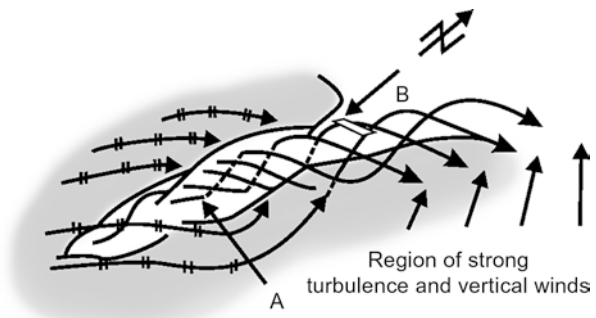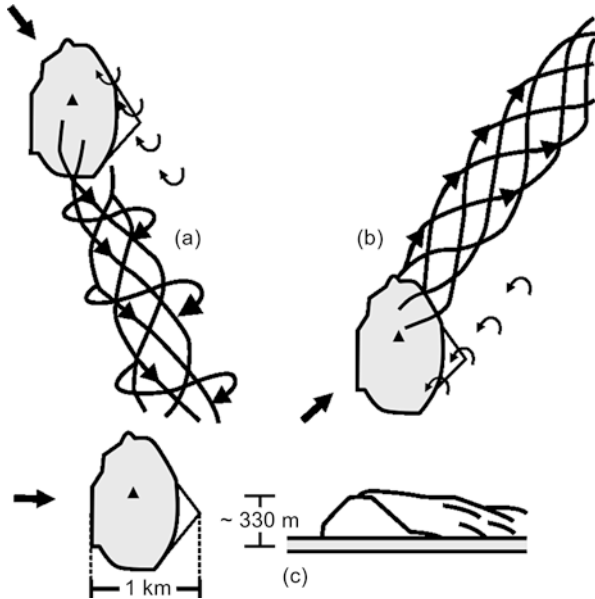Region of strong turbulence and vertical winds

Figure 7.9 A screw formed vortex street behind Ailsa Craig, Scotland.

The figure shows how vortex streets are formed in North-westerly winds and also South-westerly winds, causing difficult sailing conditions for smaller vessels on the Eastern side of the island. When there is a westerly wind only increased regular turbulence is experienced.

In order to determine the wind speed along an electric overhead line running in such terrain where significant vortex shedding may occur, it is necessary to evaluate point values that may significantly influence the wind speed at certain construction sites (tower or span) along the line on the leeward side of a steep hillside. An example is shown of a terrain with a steep side along a ridge in Figure 7.10. The topography is outlined with contour lines and locations relative to the construction point, P. Across the mountain ridge a cross section is described in Cigré TB 410 where the maximum declination angle αmax(θ)>30° occurs within specific sectors. The limiting cross sections are therefore defined to be located where the declination angle of the terrain is crossing this value of 30°. Eight main directions of the wind (N, NE, E, SE, S, SW, W and NW) are used to determine the wind at the specific site.

Such wind phenomena are well known from many countries, and TB 410 refers to Japan, New Zealand, Iceland and Norway, however scarcely reported in literature. It is also known from the mountainous island of Tenerife (Red Electrica, personal communication).

It is beyond the scope of this chapter to give a complete set of instructions how to deal with such winds, and the reader is referred to Cigré TB 410 for further information. However, a brief application example from the TB 410 is summarised in the following.
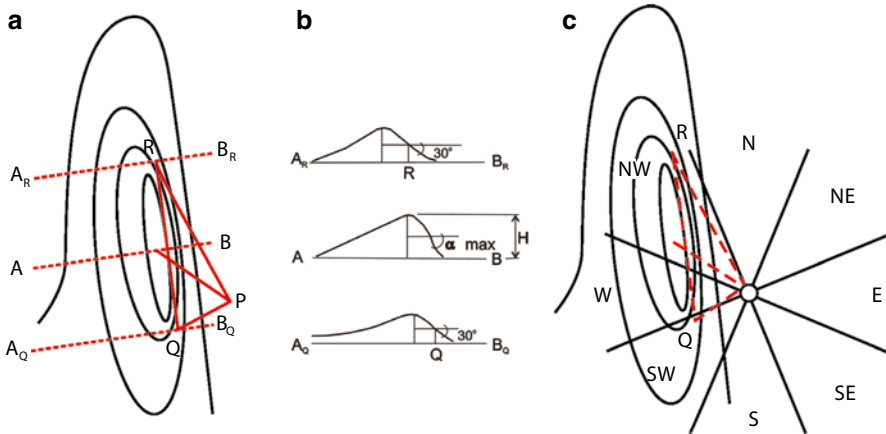
Figure 7.10 Example of steep terrain (*grey contour lines*) with possible wind gust enhancements at a construction point P. (**a**) shows the map, (**b**) vertical cross sections at three different sections, and (**c**) map with directional sectors seen from P.

Figure 7.11 shows the right-of-way of a new 132 kV line from a planned wind farm on an island in Northern Norway. This island is known to have extreme wind conditions, in particular behind the steep and sharp mountains on the island. The map shows that there are two areas with such rugged mountains, one in the northern part (points 1–2) and another and bigger in the southern part (points 3–4), on the windward side relative to the transmission line. In between them there is a plain area where the line is fully open to the Norwegian Sea towards west (left in the map).

The northern part consists of mountains mostly in the 200–300 m levels, but some peak up to the 400–500 m level. The southern part consists of somewhat higher peaks. Several of them are above 600 m asl.

The distances between the steep mountain sides and the line are typically 1–4 km.

The standard reference 10 minute average wind, 10 m above ground, is given by the wind code to be 29 m/s for this area. By applying the method described in Cigré TB 410 gust wind speeds of 55 m/s may be expected at 10 m height and 60 m/s at 20 m height in those areas where vortex streets may occur (1–2 and 3–4 in the map).

Further and updated information will be available in a new report from Cigré WG B2.28 on "Meteorological data and analyses for assessing climatic loads on OHLs" (Cigré TB 645, 2015).

7.3   Atmospheric Icing

7.3.1   Overview

Atmospheric icing may often be the most important single parameter for mechanical design of overhead lines, and also the most important weather element for disturbances in the operation of electric networks. A recent (February 2014) example

Figure 7.11 Right-of-way for a 132 kV line (*red line*) from a planned wind turbine park (Point 1) to a substation at Point 4. (The map is provided by the engineering company Jøsok Posjekt AS, Bergen, Norway.)
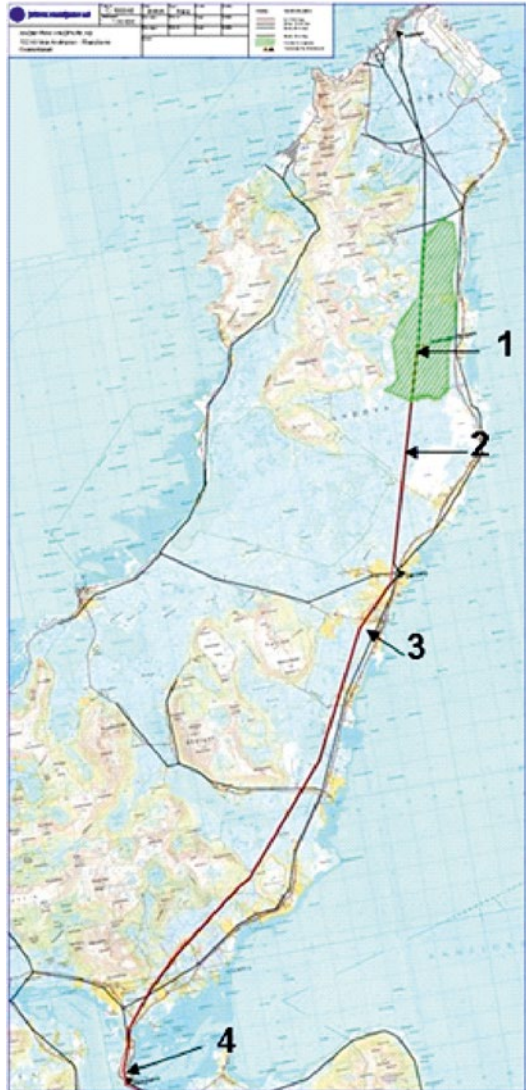
from Slovenia is shown in Figure 7.12. The Slovenian costs resulting from this icing storm damage was estimated to about € 500 million (F. Jakl, personal communication).

An example of rime icing from a high level mountain (1 400 m above sea level) is shown in Figure 7.13.

Atmospheric icing is described in great details in the Cigré TB 291 "Guidelines for meteorological icing models, statistical methods and topographical effects" (WG B2.16.03, 2006) and Cigré TB 179 "Guidelines for field measurements of ice loadings on overhead line conductors" (WG 22.06.01, 2001). It will also be updated

Figure 7.12 Freezing rain event in Slovenia February 2014 (Photo: F. Jakl).

Figure 7.13 Rime icing on a 420 kV line in Norway, 1400 m above sea level (Photo: S.E. Hagen).

with more recent knowledge and additional information in a new report from Cigré WG B2.28 on "Meteorological data and analyses for assessing climatic loads on OHLs" (soon to be published). The European COST Action 727 "Atmospheric icing on structures" have delivered a state-of-the-art report on atmospheric icing in Europe (Fikke et al. 2006).

7.3.2 Icing Processes

Atmospheric icing is a general term for several types of ice accretion as described in details in (Cigré TB 179) and (Cigré TB 291). Atmospheric icing includes in-cloud icing (hard rime and soft rime), precipitation icing (wet snow and freezing rain) and hoar frost. Often ice accretion is a mixture of two or more types (soft rime, hard rime and wet snow) depending on variations in the meteorological parameters during the icing event. Various shapes, densities, adhesion strengths, etc. result accordingly, see Table 7.2.

Glaze ice occurs in a temperature inversion situation in valleys on calm warm fronts. Raindrops in the warm (above 0 °C) air region can fall through a few hundred meters of sub-zero air to ground level. The raindrops are then super-cooled, i.e. still in the liquid phase but at sub-zero temperatures e.g. −1 to −5 °C.

On contact with a physical object, which may be an overhead line or tower structure, the raindrops freeze rapidly with virtually no trapped air within the accretion. Glaze icing produces the densest form of icing – a typical density being 900 kg/

Table 7.2 Classification of ice types with typical density ranges (Cigré TB 179)

Ice and snow type	Density (kg/m³)	Description
Glaze ice	700–900	Pure solid ice, sometimes icicles underneath the wires. The density may vary with the content of air bubbles. Very strong adhesion and difficult to knock off.
Hard rime	300–700	Homogenous structure with inclusions of air bubbles. Pennant shaped against the wind on stiff objects, more or less circular on flexible cables. Strong adhesion and more or less difficult to knock off, even with a hammer.
Soft rime	150–300	Granular structure, "feather-like" or "cauliflower-like". Pennant shaped also on flexible wires. Can be removed by hand.
Wet snow	100–850	Various shapes and structures are possible, mainly dependent on wind speed and torsional stiffness of the conductor. When the temperature is close to zero it may have a high content of liquid water, slide to the bottom side of the object and slip off easily. If the temperature drops after the accretion, the adhesion strength may be very strong.
Dry snow	50–100	Very light pack of regular snow. Various shapes and structures are possible, very easy to remove by shaking of wires.
Hoar frost	<100	Crystal structure (needle like). Low adhesion, can be blown off.

m^3 – and high ice loads are reached within hours. Icicles are often seen below the conductors as the raindrops freeze as they run off the lines. A typical picture of glaze ice is shown in Figure 7.14. The widely reported Canadian ice storm of January 1998 was due to glaze icing. Glaze icing may also result from in-cloud icing when the in-flux of cloud water is very high (Poots 1996).

Rime ice accretion occurs when small, super cooled water droplets (~10 μm) travel along with the wind flow in temperatures typically below −5 °C, and freeze spontaneously on contact with a physical body. The accretion formed is often strongly asymmetric with leading vanes into the wind direction, see Figure 7.15). This type of icing is often referred to as "in-cloud" icing and is common in hilly areas over the cloud base. The density of rime varies depending on the size and speed with which the water droplets freeze. Hard rime ranges in density from 300 to 700 kg/m³ while soft rime has densities of 150–300 kg/m³. Figure 7.16 depicts the dependency of droplet diameter on temperature for various types of accretion. Ice loads take days or even weeks to reach damaging levels. Rime ice often accretes more rapidly on small conductors or sharp edges.

Figure 7.14 Glaze ice in Slovenia February 2014. An "ice casting" of the conductor can be seen in the middle (Photo: F. Jakl).

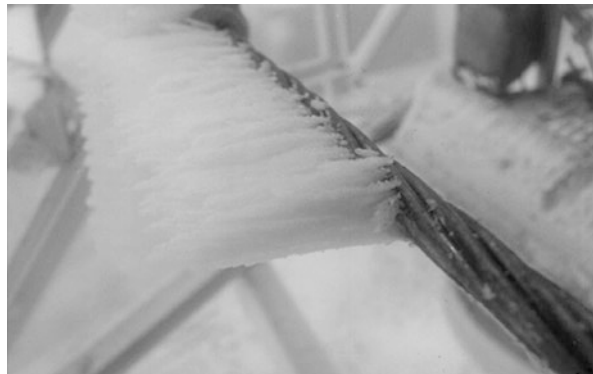**Figure 7.15** Rime icing vane (Wareing 1999).

Figure 7.16 Ice accretion type as a function of temperature and droplet size (Kuriowa 1965).
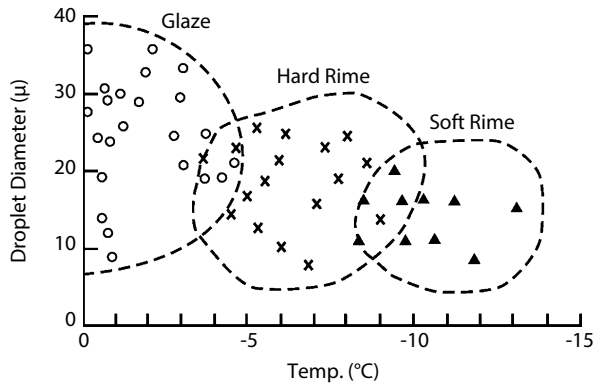

Figure 7.17 Wet snow accretion on overhead conductor (Courtesy Landsnet, Iceland).

Wet snowflakes occur as ice crystals suspended in a liquid water matrix at temperatures just above the freezing point, usually between 0,5 and 2 °C. At liquid water contents (LWC) between 15 and 40 % the flakes adhere readily to objects. They can reach a terminal velocity which is less than the local wind speeds. At LWC levels below 15 % the snow often fails to accrete on structures and lines but can penetrate into motors or other components. At LWC levels above 20 % the accretion often falls off objects.

The force of the wind compresses the snow on the surface and the accretion will become more compacted over time, meaning the porosity will decrease and density value as high as 850 kg/m³ may be reached within the deposit. This phenomenon does not increase the overall snow load on the conductor but will affect only its density. A process of circular accretion can lead to very high loads being reached in a matter of hours, see Figure 7.17.

Many meteorological parameters are significant in relation to icing accretions. Table 7.3 shows the meteorological parameters associated with each icing type with those having the greatest influence denoted "■" and those with less influence denoted "□".

Table 7.3 Meteorological parameter associated with each icing type. Those that have greatest influence are denoted "■", those with less influence "□"

Type of icing	Precipitation icing		In-cloud icing			
	Glaze due to freezing rain	Wet snow accretion	Dry snow accretion	Glaze due to super cooled cloud/fog droplets	Hard rime	Soft rime
Wind speed	■	■	□	■	■	■
Air temperature	■	■	□	■	■	■
Precipitation	■	■	■			
Liquid water content of air	■				■	■
Water droplet size	■			■	■	■
Relative humidity	■	□		■	■	■
Liquid-water content of snowflake		■	■			
Snow flake size		■	■			

Some of these parameters are contained and recorded in the general observed parameters, and others are not. The parameters generally observed are the weather, air temperature, relative humidity, precipitation (precipitation intensity), wind speed, and wind direction. Moreover, some cases may include cloud type, cloud amount, cloud base and visibility. On the other hand, among the parameters which are not generally observed, the super cooled liquid-water content of air, distribution of the volume diameter (particularly mean volume diameter) of super cooled fog/cloud droplets, liquid-water content of snowflakes, etc. have a significant influence on the icing phenomena.

In order to estimate ice loads, several physical and empirical models have been developed for glaze due to freezing rain, including icicle growth, in-cloud icing and for snow accretion. Their application depends strongly on the availability of the meteorological parameters required as an input to the models.

7.3.3   Measuring Ice Loads

Ice loads are measured in many ways, mainly depending on prevailing icing type, but also from historic reasons. Such devices are described in Cigré TB 291, Fikke et al. (2006) and WG B2.28 (Cigré TB 645, 2015).

In Canada there has been an extensive measuring program for freezing rain since 1974 (Cigré TB 291) with the so-called "Passive Ice Meter" shown in Figure 7.18 (Cigré TB 291).

In Russia regular weather stations have been equipped with special designed racks for icing measurements since the 1940's – 1950's, as shown in Figure 7.19 (WG B2.28 Cigré TB 645, 2015).

Figure 7.18 Passive Ice Meter used for measuring freezing rain in Canada (Cigré TB 291).
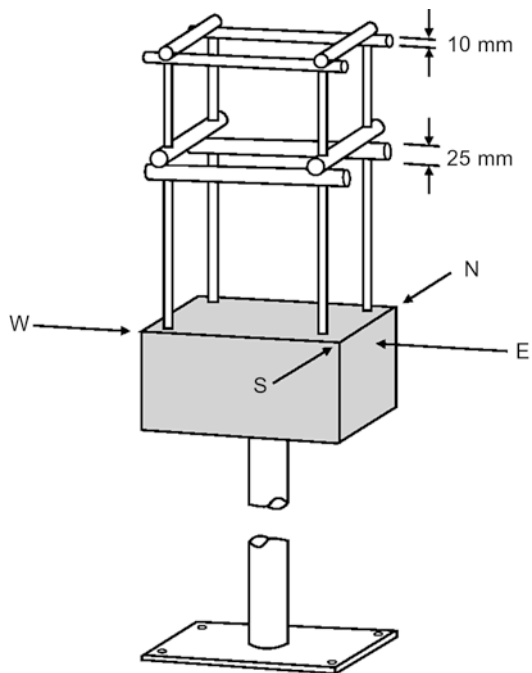

Figure 7.19 An icing rack from a Russian weather station (Courtesy S. Chereshnyuk, NTC-Power).

Some countries are using test spans, for instance in Iceland (measured since 1972) as shown in Figure 7.20 (Cigré TB 291).

In Norway a test rack, see Figure 7.21, was used to measure rime icing through the 1980's and 1990's (Cigré TB 291).

For instance in the UK a test site is established for icing measurements and hardware studies on the mountain Deadwater Fell, see Figure 7.22. Another test span is the Hawke Hill test site, Newfoundland in Figure 7.23 (CEA 1998).

Test spans like those in Figures 7.22 and 7.23 are especially useful for testing non-conventional conductor types as well as any type of hardware that may be exposed to extreme weather impacts.

7.3.4   Icing Models

Most of the following text is taken from (Cigré TB 291). However, as there have been quite substantial developments in the modelling of atmospheric icing, new opportunities have emerged by using modern weather forecasting models where icing models are embedded, see for instance (Fikke et al. 2012), (Nygaard et al. 2011) and (Nygaard et al. 2013).

Figure 7.20   Test span for icing measurements in Iceland. Many of these are mounted in orthogonal pairs, each span 80 m long (Courtesy Landsnet).

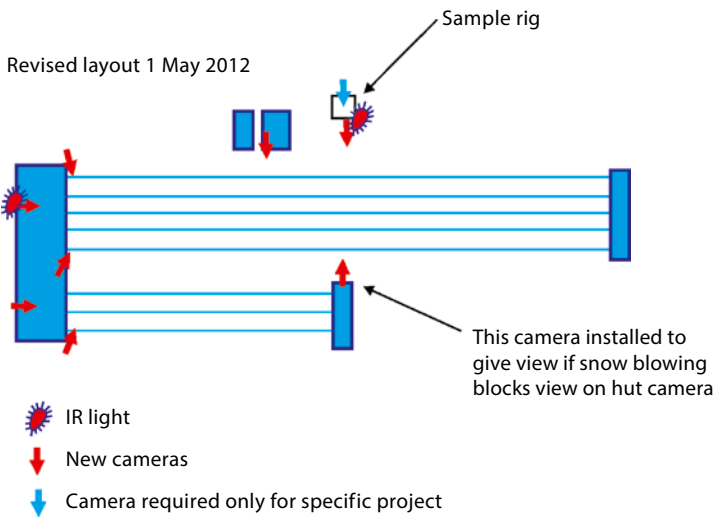**Figure 7.21** Rack for measuring rime icing in Norway (Photo: B.E.K. Nygaard).

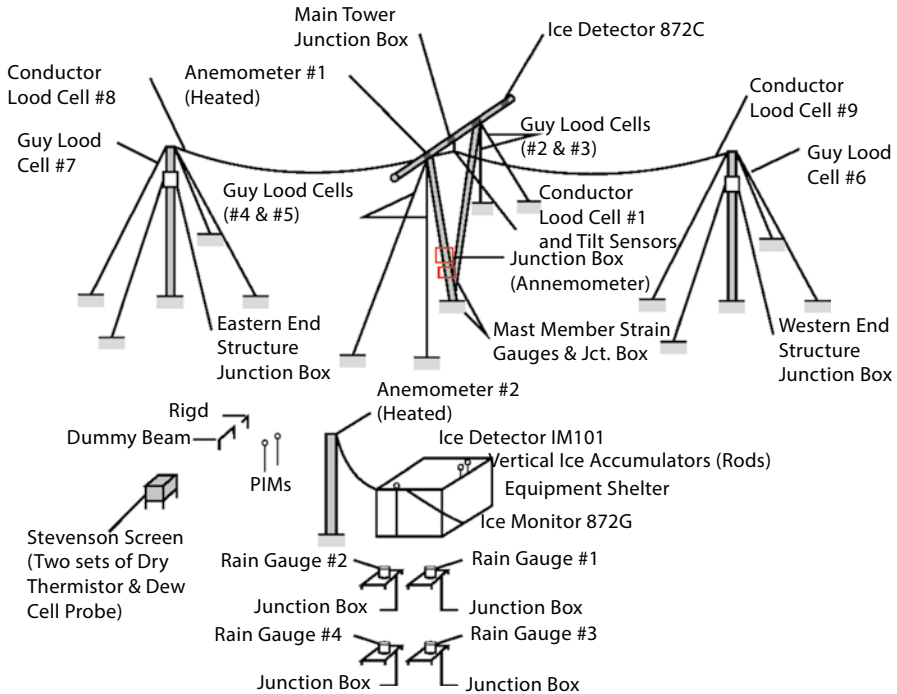**Figure 7.22** Layout of new Deadwater Fell test site (Courtesy J.B. Wareing).

Figure 7.23 Hawke Hill test site, Newfoundland (Haldar 2007).

The use of icing models to provide ice load data is obviously attractive. They give an estimation of ice loads for defined conductors and are often restricted to a particular type of icing.

Estimating ice loads on conductor from models based on atmospheric data is a complex process involving:

- source of moisture (maritime air)
- cloud formation
- precipitation (for precipitation icing)
- liquid water content (LWC) in air (for in-cloud icing)
- terrain effects
- collision of drops or droplets with the ice surface
- accretion rate
- torsional rigidity effects
- change in accreting surface characteristics (size, roughness, shape)
- ice shedding
- local temperature/wind effects.

The selection of icing models is therefore dependent upon icing processes as described above. Some icing models use relatively simple approaches and are restricted to a particular type of icing, while others start from more fundamental equations and

can address a range of icing types. Icing models may be used both to estimate ice loads for defined conditions and to compute icing statistics from a historical database of meteorological conditions. In most cases, essential input parameters such as LWC and droplet sizes are, in general, not available from a climate database and must be estimated from the available meteorological parameters.

It is beyond the scope of this chapter to give a complete description of the various icing models. The reader is referred to the International Standard ISO 12494 (ISO 2001), Cigré TB 291 and the WG28 report for more details on especially freezing rain (glaze ice) and in-cloud icing (rime ice). In the case of wet snow there has been some significant development in years which are only recently published and therefore not so widely known. The following text is mainly excerpts from Nygaard et al. (2013).

> *Ice accretion modelling – state of the art on wet snow models* (WG B2.28 Cigré TB 645, 2015).

Different variations of simple cylindrical accretion models for wet snow are found in the literature (Finstad et al. (1998), Sakamoto and Miura (1993), Admirat (2008), Makkonen and Wichura (2010), Nygaard et al. (2013)). The basics of these models can be described with the following equation

$$\frac{dM}{dt} = \beta \, V \, w \, A \tag{7.1}$$

where dM is the accumulated snow mass per unit length during the time step dt, β is the sticking efficiency (the fraction of snow that sticks to the cylinder after collision), A is the cross-sectional area of the cylinder perpendicular to the snowflake impact speed V, while w is the mass concentration of wet snow in the air. The snowflake impact speed is the vector sum of the wind speed U and the terminal velocity of the snowflakes v_s:

$$V = \sqrt{U^2 + v_s^2} \tag{7.2}$$

The time dependent model is called a cylindrical model because it assumes that the snow deposit maintain its cylindrical shape.

Given meteorological data at a temporal resolution of Δt, (Eq. 7.1) can be numerically integrated forward in time, assuming that the meteorological conditions are constant within Δt. The integration scheme can be found in e.g. Nygaard et al. (2013)

Since w is not directly measured at regular weather stations, methods to estimate w based on the standard meteorological variables have been suggested. The most widely used parameterization relies on the measured water equivalent precipitation intensity at the ground P and the terminal velocity of the falling snowflakes v_s (Admirat 2008), by $w = P/v_s$. Another approach used by Makkonen and Wichura (2010) is to estimate w from observed visibility V_m by a formula presented in Makkonen (1989): $w = 2100 V_m^{1.29}$.

The sticking efficiency β, is introduced in order to account for the bouncing effect of snowflakes after collision with the cylinder. Due to the general lack of sufficient and precise wet snow measurements as well as limitations in the physical understanding of the collision process, a precise formula for this coefficient has not been

attainable. However, simple empirical relations have been suggested based on both limited field studies and laboratory experiments (Finstad et al. (1998); Sakamoto and Miura (1993); Sakamoto (2000); Admirat (2008)). A commonly used parameterization has been a simple inverse relation to the wind speed by $\beta = 1/U$ (Admirat 2008). This was adopted in the international standard for atmospheric icing of structures (ISO-12494 2000), but its uncertainty is clearly underlined:

*Estimation of the sticking efficiency β of wet snowflakes is presently quite inaccurate. $\beta = 1/U$ should be seen only as a first approximation until more sophisticated methods to estimate β have been developed (*ISO-12494 2000*).*

A more recent calibration of the sticking efficiency has been published in Nygaard et al. (2013). By using 50 years of wet snow measurements, where many occurred during windy conditions, they showed that $\beta = 1/U^{0.5}$ gave a much better match with observations compared to the original approximation. Consequently, the parameterization described in Nygaard et al. (2013) is recommended unless sufficient amount of empirical data supports other methods or calibration factors.

For the density of the accreted snow ρ_s, it is recommended to use a formula on the form $\rho_s = k + 20\ U$, where k must be determined according to local conditions. Admirat (2008) found $k = 300$ based on some documented cases of wet snow in Japan, while including cases from France k was closer to 200. The density should however be limited to a maximum of roughly 750 kg/m³, which is the highest reported in field studies (Eliasson et al. 2000).

7.3.5 Identification of Wet Snow

Identification of wet snow conditions has been discussed in the literature. Admirat (2008) assumed that all precipitation reaching the ground at 2-m temperatures between 0 °C and 2 °C was in the state of wet snow. Sakamoto (2000) used a somewhat similar criterion but found an upper temperature limit that changed with altitude and weather condition prevailing during the storm. Makkonen (1989) emphasized the role of atmospheric moisture for the presence of wet snow, and showed that one necessary condition was a positive wet-bulb temperature (Tw > 0 °C).Nygaard et al. (2014) identified the wet-bulb temperature interval between 0 °C and 1.2 °C as favourable conditions for wet snow accretion.

7.3.6 Application of Numerical Weather Prediction Models

The icing models described above deals with the physical accretion processes on the conductors, where the input parameters are known or can be anticipated with an acceptable accuracy. However, when the input parameters are not known or can be assessed indirectly from other sources, it has now become possible to generate parameters like liquid water content, cloud droplet sizes, and wet snow content in the air from regular numerical weather prediction models, see Fikke (2005), Nygaard et al. (2011), Fikke et al. (2012), Nygaard et al. (2013) and Nygaard et al. (2014).

Such models are useful for case studies, studies of design loads (climatology) and mapping of ice loadings for wet snow and rime ice loads. The numerical weather prediction models are still not fully reliable for forecasting low level temperature inversions and hence freezing rain.

A recent example is the ice load map developed for United Kingdom shown in Figure 7.24 (Nygaard et al. 2014). The map data are given with a resolution of 500 m × 500 m, and the overhead line designer can therefore enter the geographical coordinates into the data base and directly get the ice loads as well as the wind speeds and combined wind and ice loads to be used as design parameters for the specified line with the same resolution.

As can be seen from Figure 7.24, the ice loadings are specified in kg/m up to 10 kg/m. In the higher mountains, mainly in the Scottish Highlands, the rime ice loads may locally be higher or lower due to smaller scale variations in the topography where local conditions may increase or reduce the icing intensities.

This procedure is also included in the WG B2.28 Cigré TB 645 2015.

Figure 7.24 Combined wet snow and rime ice load map for the United Kingdom. Color code in *upper right corner* (Nygaard et al. 2014).
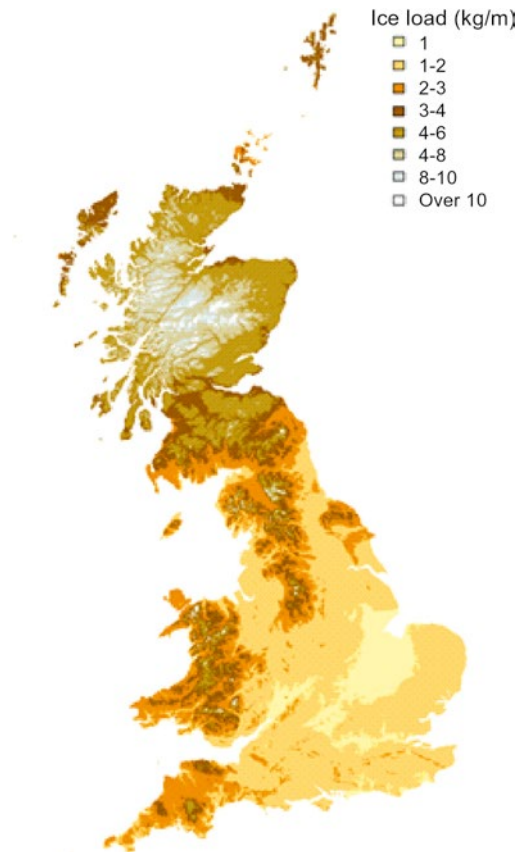
7.4   Other Topics

7.4.1   Combined Icing and Pollution

Pollution on insulators is well known both for sub-stations and for overhead lines. Such pollution may cause leakage currents and eventually flashovers for electrical equipment in industrial or coastal areas. Such pollution may be due to industrial dust, fine sand from deserts and spray of sea salt from oceans under strong wind conditions (over sea).

However, sea salt and industrial pollution may also act as condensation nuclei for droplets in clouds, far away from their origin. Under freezing conditions such droplets may freeze on insulators on overhead lines in mountains relatively far away from the coast line or industrial source as well. Flashovers due to this reason are reported in Fikke et al. (1993).

7.4.2   Effects from Changes in Global Climate

The Intergovernmental Panel on Climate Change (IPCC) issued in 2013 the first WG report to the Fifth Assessment Report on climate change in 2013 (IPCC 2013). This report discusses the scientific basis, and their main conclusion is a confirmation of the findings of the Fourth assessment report in 2007 (IPCC 2007). Due to various human activities the emissions the content of CO_2 is steadily increasing to record high levels and currently reaching the 400 ppm level, according to IPCC (2013) (See Figure 7.25).

Figure 7.26 shows the observed global mean combined land and ocean surface temperature anomalies, from 1850 to 2012 from three data sets. The top panel shows annual mean values. Bottom panel shows decadal mean values including the estimate of uncertainty for one dataset (black). Anomalies are relative to the mean of 1961–1990.
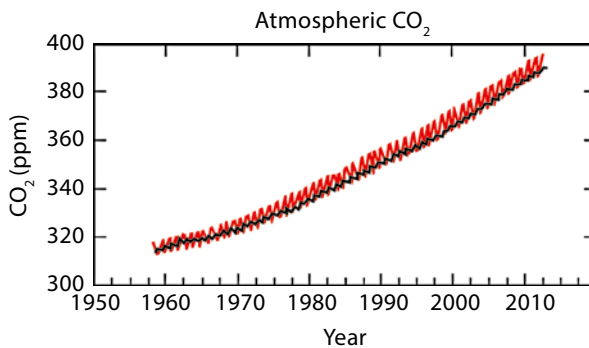

Figure 7.25   Increase in CO_2 in the atmosphere since 1958. *Red curve*: Mauna Loa, Hawaii, and *black curve*: South Pole.
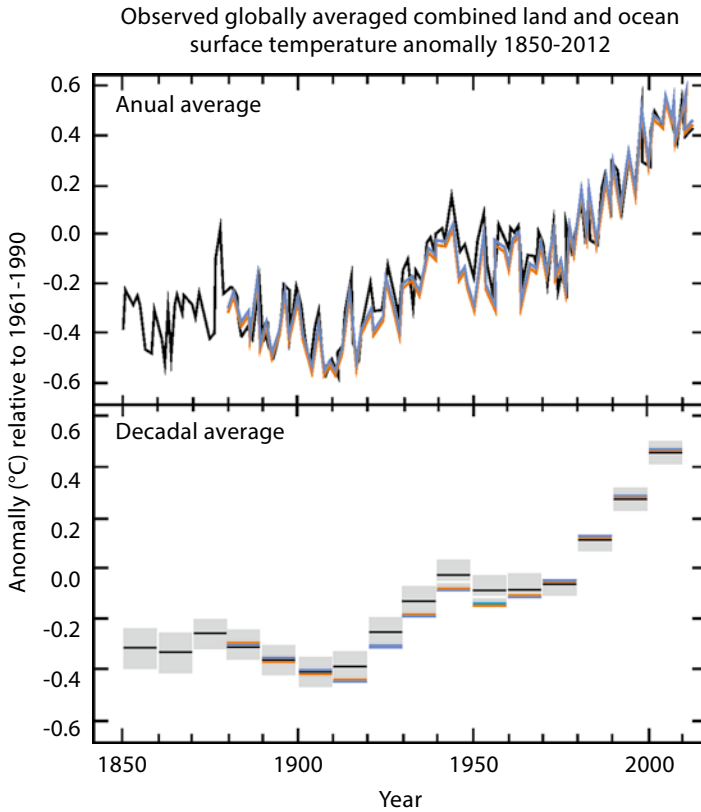
Figure 7.26 Observed global mean combined land and ocean surface temperature anomalies, from 1850 to 2012 from three data sets. *Top panel*: annual mean values. *Bottom panel*: decadal mean values including the estimate of uncertainty for one dataset (*black*). Anomalies are relative to the mean of 1961–1990.

As can be seen from Figure 7.26 the global temperature is constantly increasing on a decadal scale, although there are several shifts in global temperatures on the scale of a few years. The other sub-reports from IPCC Working Groups II and III were published in 2014 (WG II Impacts, Adaptation and Vulnerability) (IPCC 2014, WGII) and (WG III Mitigation on Climate Change) (IPCC 2014, WGIII). The Synthesis Report will be published in October 2014.

In 2012 IPCC also issued a Special Report on Managing the Risks of Extreme Events and Disasters to Advance Climate Change Adaptation (IPCC, SREX 2012). As the title implies, this Special Report discusses the potentials of extremes of various weather phenomena in a warming atmosphere on a global scale, although with some regional examples.

In order to identify potential consequences for the international electric overhead industry it is necessary to look into more detailed reports where climate parameters are downscaled to a more regional and local scale. One such study for Europe was

published in 2013 by the Norwegian Meteorological Institute, together with the Norwegian Academy of Science and Letters, in cooperation with the European Academies Science Advisory Council (easac) (NMI and DNVA 2013).

Another report was issued in February 2014 entitled: "Climate Change. Evidence & Causes. An overview from the Royal Society and the US National Academy of Sciences". (Roy. Soc. and NAS 2014). This report is structured as Question and Answers. As a summary to Q. 13 "How does climate change affect the strength and frequency of floods, droughts, hurricanes and tornadoes?" the report says:

> *Earth's lower atmosphere is becoming warmer and moister as a result of human-emitted greenhouse gases. This gives the potential for more energy for storms and certain severe weather events. Consistent with theoretical expectations, heavy rainfall and snowfall events (which increase the risk of flooding) and heatwaves are generally becoming more frequent. Trends in extreme rainfall vary from region to region: the most pronounced changes are evident in North America and parts of Europe, especially in winter.*

It should be emphasized that regional studies like those mentioned above will constantly be published in most regions of the world. It is therefore not within the scope of this chapter to give a complete overview of reports of this kind, since such a summary may soon be incomplete or outdated. Any utility or other authority is recommended to review the available information locally whenever needed.

According to Fikke (2011) utilities in many countries have already incorporated precautions or considering adaptations for mitigating potential effects relating to their networks. Some of the most important findings were (name of informant is given in parentheses):

Canada, BC Hydro (J. Toth): Temperature increase will lead to higher beetle infestation, drier summers (fire risks, slope instability), more woodpeckers, changes in peak load patterns, etc. Higher precipitation rates may lead to river erosion and flooding, mudslides, increased corrosion, higher frequency and severity of wind and ice storms, hail storms and reduced opportunity for live-line work. Wind effects may affect the failure rates, recovery time and reliability, vegetation control practices and withstand levels of hardware. Other effects to be considered are: rising sea level (for coastal substations), melting permafrost, increased lightning activities, fog, in-cloud icing and transmission line ratings.

Australia (H. Hawes): Expected effects are mainly related to extreme storm intensities, rainfall intensities, insulator pollution, wildfire (bush fire) risk, etc.

United Kingdom (J.B. Wareing): Main focus areas are change in risks for high wind and wet snow accretion, thermal rating and changes in seasonal demands due to increased use of air conditioning.

Russia (S. Chereshnyuk): Melting of permafrost, flooding and landslides, wind loads may increase in some regions (and decrease in others).

Norway (S.M. Fikke): Wet snow and rime icing may increase in some areas and decrease in others, higher avalanche risks in many areas, reduced weather windows for helicopter operation for maintenance.
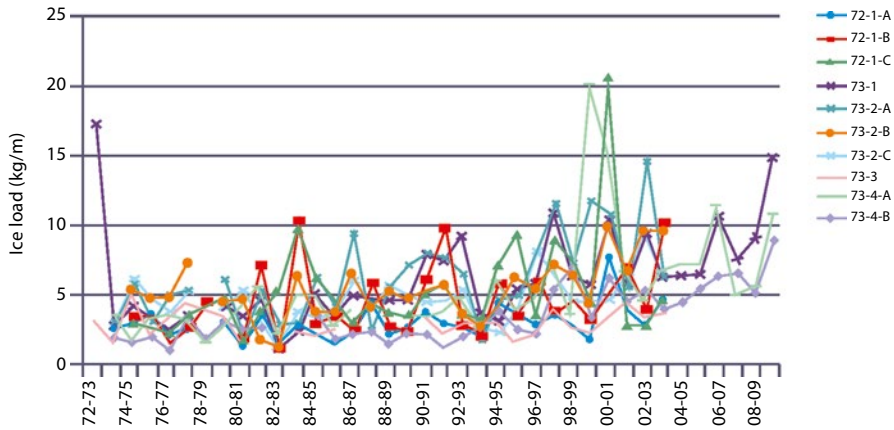
Figure 7.27   39 years of measurements of ice loadings on 10 different test spans in Iceland.

Iceland (Á. J. Elíasson): After 39 years of measurements it seems to be a small, but increasing trend in recorded ice loads since 1995, as shown in Figure 7.27.

TB 291 also mentions some potential developments for atmospheric icing, although the high uncertainties are strongly emphasized:

> *Wet snow: More seldom in coastal low-lands, but maybe more often on coastal mountains. For inland areas with a cold climate wet snow may increase in frequency and intensity at all levels.*
>
> *Rime ice: Risk of rime ice may decrease in lower levels and increase in higher levels.*
>
> *Freezing rain: Not possible to evaluate with current knowledge.*

For tornadoes there are no trends identified in the literature. Global climate models do not show correlations between tornado frequency and global climate variations (valid for both the US and Australia) (Fikke 2011).

References

Admirat, P.: Wet snow accretion on overhead lines. In: Farzaneh, M. (ed.) Atmospheric Icing of Power Networks, pp. 119–169. Springer, Dordrecht (2008)

ASCE: Manual 74 "Guidelines for Electrical Transmission Line Structural Loading". ASCE, Reston (2009)

CAN/CSA Standard C22.3 No. 1–10 Overhead Systems (2010)

CEN EN 1991–1 Actions on Structures – General Actions, Brussels

Cigré WG B2.28 TB 645 Meteorological Data and Analyses for Assessing Climatic Loads on OHLs (2015)

Elíasson, Á.J., Thorsteins, E., Ólafsson, H.: Study of wet snow events on the southcoast of Iceland. In: Proceedings of 9th International Workshop on Atmospheric Icing of Structures (IWAIS), Chester (2000)

EPRI.: EPRI Transmission Line Reference Book – 115–345 kV Compact Line Design. EPRI (2008)

Fikke, S.M.: Impact of climate change on transmission systems. Cigré SC B2 Tutorial 05 July 2011, Reykjavik

Fikke, S.M., Hanssen, J.E., Rolfseng, L.: Long range transported pollutants and conductivity of atmospheric ice on insulators. IEEE Trans. Power Deliv. **8**(3), 1311–1321 (1993)

Fikke, S.M.: Modern meteorology and atmospheric icing. In: Proceedings of 11th International Workshop on Atmospheric Icing of Structures (IWAIS), Montreal (2005)

Fikke, S.M., Ronsten, G., Heimo, A., Kunz, S., Ostrolizlik, M., Persson, P.E., Sabata, J., Wareing, B., Wichura, B., Chum, J., Laakso, T., Säntti, K., Makkonen, L.: COST 727: Atmospheric icing on structures. Measurements and data collection on icing: State of the art. MeteoSwiss Publication # 75, 110p (2006)

Fikke, S., Nygaard, B.E., Horsman, D., Wareing, J.B., Tucker, K.: Extreme Weather Studies by Using Modern Meteorology, Cigré Session Paper B2-202. Cigré, Paris (2012)

Finstad, K., Fikke, S.M., Ervik, M.: A comprehensive deterministic model for transmission line icing applied to laboratory and field observations. In: Proceedings of 4th International Workshop on Atmospheric Icing on Structures (IWAIS), Paris, pp. 227–231 (1998)

Haldar, A.: Twenty years of ice monitoring experience on overhead lines in Newfoundland and Labrador. IWAIS XII, Yokohama (2007)

IEC TR 60826 Designing criteria for overhead transmission lines, IEC (2003)

IEEE: Standard 524 "Guide to the Installation of Overhead Transmission Line Conductors". IEEE, New York (2003)

IPCC: In: Solomon, S., Qin, D., Manning, M., Chen, Z., Marquis, M., Averyt, K.B., Tignor, M., Miller, H.L. (eds.) Climate Change 2007: The Physical Science Basis. Contribution of Working Group I to the Fourth Assessment Report of the Intergovernmental Panel on Climate Change. Cambridge University Press, Cambridge, UK/New York (2007). 996 pp

IPCC: Summary for policymakers. In: Field, C.B., Barros, V.R., Dokken, D.J., Mach, K.J., Mastrandrea, M.D., Bilir, T.E., Chatterjee, M., Ebi, K.L., Estrada, Y.O., Genova, R.C., Girma,

B., Kissel, E.S., Levy, A.N., MacCracken, S., Mastrandrea, P.R., White, L.L. (eds.) Climate Change 2014: Impacts, Adaptation, and Vulnerability. Part A: Global and Sectoral Aspects. Contribution of Working Group II to the Fifth Assessment Report of the Intergovernmental Panel on Climate Change, pp. 1–32. Cambridge University Press, Cambridge, UK/New York (2014a)

IPCC: Summary for policymakers. In: Edenhofer, O., Pichs-Madruga, R., Sokona, Y., Farahani, E., Kadner, S., Seyboth, K., Adler, A., Baum, I., Brunner, S., Eickemeier, P., Kriemann, B., Savolainen, J., Schlomer, S., von Stechow, C., Zwickel, T., Minx, J.C. (eds.) Climate Change 2014, Mitigation of Climate Change. Contribution of Working Group III to the Fifth Assessment Report of the Intergovernmental Panel on Climate Change. Cambridge University Press, Cambridge, UK/New York (2014b)

IPCC Climate Change.: The Physical Science Basis. Summary for Policymakers. WG I Contribution to the Fifth Assessment Report of the Intergovernmental Panel on Climate Change. www.clima-techange2013.org (2013)

IPCC SREX.: Managing the Risks of Extreme Events and Disasters to Advance Climate Change Adaptation. A Special Report of Working Groups I and II of the Intergovernmental Panel on Climate Change. Cambridge University Press, Cambridge, UK/New York. www.ipcc.ch (2012)

ISO 12494 Atmospheric icing on structures, Geneva (2001)

Kuroiwa, D.: Icing and Snow Accretion on Electric Wires, U.S. Army CRREL Report, 17–3, p. 10 (1965)

Makkonen, L.: Estimation of wet snow accretion on structures. Cold Reg. Sci. Technol. **17**, 83–88 (1989)

Makkonen, L., Wichura, B.: Simulating wet snow loads on power line cables by a simple model. Cold Reg. Sci. Technol. **61**(2–3), 73–81 (2010)

NESC: National Electrical Safety Code. IEEE, New York (2007)

Norwegian Meteorological Institute (NMI) and DNVA.: Extreme weather events in Europe: preparing for climate change adaptation. (Can be downloaded from www.dnva.no) (2013)

Nygaard, B.E.K., Kristjánsson, J.E., Makkonen, L.: Prediction of in-cloud icing conditions at ground level using the WRF model. J. Appl. Meteorol. Climatol. **50**(12), 2445–2459 (2011)

Nygaard, B.E.K., Ágústsson, H., Somfalvi-Tóth, K.: Modeling wet snow accretion on power lines: improvements to previous methods using 50 years of observations. J. Appl. Meteorol. Climatol. **52**, 2189–2203 (2013)

Nygaard, B.E.K., Seierstad, I.A., Veal, A.: A new snow and ice load map for mechanical design of power lines in Great Britain. Cold Reg. Sci. Technol. (2014)

Poots, G.: Ice and Snow Accretion on Structures. Research Studies Press, Ltd, Somerset (1996)

Roy. Soc. and NAS.: Climate Change. Evidence & Causes. Royal Society (UK) and the US National Academy of Sciences. Can be downloaded from http://royalsociety.org/policy/projects/climate-evidence-causes/ (2014)

Sakamoto, Y.: Snow accretion on overhead wires. Philos. Trans. R. Soc. A. **358**, 2941–2970 (2000)

Sakamoto, Y., Miura, A.: Comparative study on wet snow models for estimation snow load on power lines based on general meteorological parameters. In: Proceedings of 6th International Workshop on Atmospheric Icing on Structures (IWAIS). Budapest, pp. 133–138 (1993)

Standards Australia AS/NZS.: AS 1170.2 SAA loading code part 2: Wind loads (1999)

Wareing, J.B.: Ice accretion loads on different conductors to apply to ETR 111 line design, EATL Report 4720, January WMO (1995) Global perspectives on tropical cyclones. TD-No. 693, Tropical Cyclone Programme Report No. TCP-38, World Meteorological Organization, Geneva (1999)

Svein M. Fikke has a M.Sc. in meteorology from the University of Oslo in Norway. His professional career ha-s been related to extreme weather impacts on infrastructure such as oil platforms, TV masts and towers, and electrical overhead lines, especially in complex mountainous terrain. He has been responsible for advising on ice and wind loadings on electrical overhead lines in Norway for 40 years, first at the Norwegian Meteorological Institute, then at the Norwegian Electric Power Research Institute and for the Norwegian TSO Statnett until retirement. After official retirement he has continued as a consultant, serving utilities both within Norway as well as in many countries abroad. He has been the Norwegian member of SC B2 and member and convenor of several working groups. Fikke received the Cigré Technical Committee Award in 2002, and has authored numerous papers in journals and to conference proceedings.